analytical
chemistry

Discovery of Environment-Sensitive Fluorescent Agonists for α1-Adrenergic Receptors

Xiaojun Qin,[†] Zhao Ma,[†,‡] Xingye Yang,[†] Shilong Hu,[†] Xinxin Chen,[†] Dong Liang,[†] Yuxing Lin,[†] Xiaodong Shi,[§] Lupei Du,[†] and Minyong Li*[,†,¶]

[†]Department of Medicinal Chemistry, Key Laboratory of Chemical Biology (MOE), School of Pharmacy, Shandong University, Jinan, Shandong 250012, China

[‡]Department of Biochemistry and Molecular Medicine, UC Davis Comprehensive Cancer Center, University of California, Davis, Sacramento, California 95817, United States

[§]Department of Chemistry, University of South Florida, Tampa, Florida 33620, United States

[¶]State Key Laboratory of Microbial Technology, Shandong University, Jinan, Shandong 250100, China

S *Supporting Information*

ABSTRACT: A series of novel fluorescent agonists were well developed herein with turn-on switch for α1-adrenergic receptors (α1-ARs) by conjugating the environment-sensitive fluorophore 4-chloro-7-nitrobenzoxadiazole with phenylephrine. Overall, these probes exhibited efficient binding and apparent fluorescence intensity changes (up to 10-fold) upon binding with α1-ARs. Moreover, these probes have been successfully applied for selectively imaging α1-ARs in the living cells. The dynamic process of α1-ARs internalization was traced successfully with these newly designed fluorescent agonists. Fluorescence polarization assay demonstrated specific interactions between these probes and α1-ARs. With these new probes, a bioluminescence resonance energy transfer binding assay has been well established and applied to the high-throughput screening of unlabeled α1-ARs agonist and antagonist. It is expected that these environment-sensitive fluorescent turn-on agonists may provide useful new tools in studying pharmacology and physiology of α1-ARs during drug discovery.
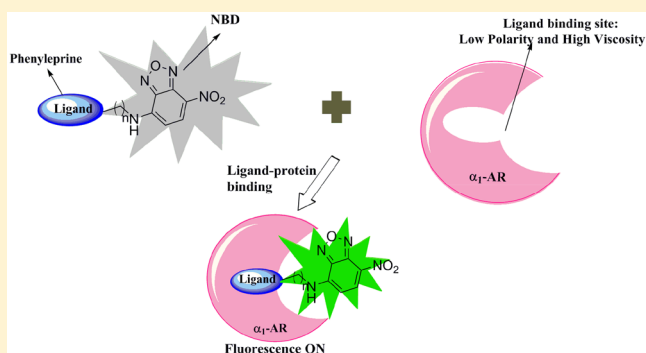
G protein-coupled receptors (GPCRs) contain seven putative transmembrane domains, which belong to the superfamily of cell-surface receptors. Approximately 40% of all current medicinal drugs targets bound up with GPCRs. It is clear that localization of target proteins is crucial for further modification, characterization, and functionalization. To ensure the befitting responses to stimuli, GPCRs usually activate with the mechanism of internalization,[1,2] which leads to desensitization. Consequently, an effective method in detecting the localization and real-time monitoring ligand-mediated internalization of receptors is of importance since it can provide the mechanistic insights for understanding the signal transduction and function of GPCRs.

With the remarkable advancement of fluorescence analysis technology, several effective fluorescent ligands have been widely used for tracking down bioactive targets, such as proteins, channels, enzymes, and GPCRs.[3−6] Comparing with other analytical methods, fluorescent ligands served as an attractive toolkit for GPCRs study with the ability to provide dynamic information on the real-time and spatial−temporal resolution for GPCRs structure and function in molecular, live cells or tissues and organisms.[7−9] During the past decade, numerous fluorescent ligands have been developed in tracing the dynamic processes of GPCRs, such as trafficking and internalization.[2,8,10] However, the high background signal is often considered as one major challenge of those reported fluorescent ligands. To overcome this obstacle, fluorescent turn-on probes have attracted more and more attention. Nowadays, it is convenient to design fluorescent probes on the basis of catalytic activity or reactive activity for enzyme targets. Nevertheless, how to branch out fluorescent turn-on probe for nonenzyme proteins, such as GPCRs, remains a challenging task.[11] One possible fluorescent turn-on design strategy is to employ fluorophores because of their ability in varying spectroscopic output based on the surrounding environment physicochemical properties. It is known that the ligand-binding sites of GPCRs are often hydrophobic with low polarity and high viscosity. Therefore, environment-sensitive turn-on fluorescence strategy can be achieved for desired GPCRs

visualization upon binding with the hydrophobic fluorescent ligands.

α_1-Adrenergic receptors (α_1-ARs) consist of seven putative transmembrane domains, which are the prominent members of the superfamily of GPCRs. It has been identified that α_1-ARs are abundantly expressed in a variety of cells, organs, and tissues and play a crucial role in mediating many physiological effects of the human body. So far, α_1-ARs are comprised of at least three subtypes (α_{1A}, α_{1B}, and α_{1D}) on the basis of their different intrinsic properties, including gene sequence, distribution in organ/tissue, and pharmacological properties.[12,13] Functional experiments manifested that α_1-ARs can respond to neurotransmitters and hormones. For example, norepinephrine and epinephrine are carrying out important roles in mediating hepatic glucose metabolism, myocardial inotropy, and chronotropy smooth muscle contraction.[13] In addition, α_1-ARs are employed as the therapeutic targets with several diseases such as hypertension, lower urinary tract symptoms (LUTS), benign prostatic hyperplasia (BPH), and prostate cancer.[3,14−16] Therefore, to further advance molecular pharmacology study and drug discovery of α_1-ARs, new effective molecular probes with diversified structure and fluorescent property are highly desired. Our lab has been working on developing effective fluorescent ligands for imaging α_1-ARs and several fluorescent ligands based on α_1-ARs antagonist phenylpiperazine and quinazoline derivatives. Those probes have extended useful tools to image and track the α_1-ARs in living cells[17−20] and living tissues and organisms.[3] Despite the powerful fluorescent technologies, it is still highly demanded to develop more formidable fluorescent turn-on ligands for dynamic changes like ligand-mediated receptors internalization of α_1-ARs. α_1-ARs are known to be internalized in response to agonists activation.[2,21]

Based on these results, we aim at developing novel fluorescent turn-on agonists, which can image localization and meanwhile real-time monitor for internalization of α_1-ARs (Scheme 1A). In this case, phenylephrine (PE),[22] an effective

Scheme 1. (A) Design of PE-NBD Environment-Sensitive Fluorescent Agonists for α_1-ARs; (B) Synthesis of the Fluorescent Agonists
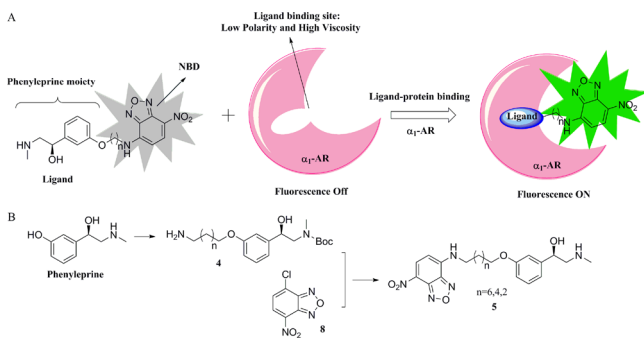
α_1-ARs agonist, was selected to bind with α_1-ARs via receptor−ligand interaction and then induce receptors internalization. The 4-chloro-7-nitrobenzoxadiazole (NBD) gives green emission when the 7-position is substituted with amine, which have been broadly used in labeling small molecules and proteins as well as advanced imaging and spectroscopy in living cells.[23−25] Furthermore, NBD is a solvatochromic fluorophore since it exhibits very low fluorescence in polar and protic environments, whereas an increasing fluorescence in hydro-

phobic environments, which could provide the highly desired high signal-to-background ratios.[11,26,27] Accordingly, NBD was selected as the environment-sensitive fluorophore for locating and tracing α_1-ARs in the current report. Subsequently, a series of PE-NBD fluorescent agonists were well synthesized and characterized. Upon binding with α_1-ARs hydrophobic ligand-binding domain, the desired fluorescent turn-on has been successfully achieved, allowing these new fluorescent agonists to be conveniently applied to the visualization, localization, and monitoring internalization of α_1-ARs in living cells without complicated steps. Meanwhile, fluorescent polarization (FP)[28−30] and bioluminescence resonance energy transfer (BRET)[23,24] assay were also conducted in characterizing the binding affinity with α_1-ARs and these fluorescent agonists. Especially, these fluorescent agonists can be applied to establish the screening assay for α_1-ARs agonists and antagonists based on the BRET assay.

■ EXPERIMENTAL SECTION

Synthesis. The convenient synthesis of PE-NBD fluorescent agonists was completed as depicted in Scheme 1B. Further detailed synthesis can be found in the Supporting Information (Scheme S1).

Measurement of Spectroscopic Properties. Probes **5a−c** was completely dissolved in DMSO as stock solution (5 mM). The stock solution was diluted by PBS (pH 7.4), water, and organic solvent including DMSO, methanol, acetonitrile, and ethanol to acquire 5, 10, 20, 30, 40, and 50 μM solutions. The UV absorbance spectra of **5a−5c** (20 and 50 μM) and fluorescence spectra were obtained on a PUXI TU-1901 spectrophotometer and a Thermo Varioskan microplate reader, respectively. Furthermore, the influence of viscosity in solution was determined by addition of glycerin (indicated in % v/v) in water with 50 μM of probes. In addition, the absolute quantum yield was investigated in PBS solution (pH 7.4) by a combined transient or steady-state fluorescence spectrometer (FLS920).

Assay to Radio-Ligand Competitive Binding. The cell membrane proteins of α_{1A}-, α_{1B}-, and α_{1D}-ARs stable transfected HEK293 cells will be prepared according to established protocol at HDB.[31,32] The membrane concentration was measured using Pierce BCA Protein Assay Kit.

Membrane Titration. The different concentrations of α_1-ARs membrane (20, 10, 5, 2.5, and 0 μg protein/well) were incubated, and [^{3}H]-prazosin (1 nM final, Cat. No. #NET616, PerkinElmer) with or without reference compound prazosin (1uM final) in assay buffer (50 mM HEPES, 1 mM CaCl$_2$, 5 mM MgCl$_2$, 0.2%BSA, pH 7.4) was kept at 37 °C for 2 h. Then the binding reaction was stopped by rapid filtration through GF/C filter plates using cell harvester. The plates well was washed three times with wash buffer (50 mM HEPES, 500 mM NaCl, 0.1%BSA, pH 7.4) and dried at 37 °C for 2 h. After adding a scintillation cocktail of 50 μL to each well, the plate-bound radioactivity was determined using Topcount NTX. Based on the results of Figure S2A, 2 μg of α_{1B}-AR, α_{1D}-AR and 5 μg of α_{1A}-AR membrane in each well was selected for the next experiment.

Saturation Binding Assay. Then, incubated [^{3}H]-prazosin (8 points, twofold dilution from 2 nM) and α_1-ARs membrane (2 μg of α_{1B}-AR, α_{1D}-AR and 5 μg of α_{1A}-AR in each well) with or without reference compound prazosin (1uM final) was kept in assay buffer at 37 °C for 2 h (Figure S2B). Then, 1 nM of [^{3}H]-prazosin was chosen for the next experiment.

Compound Test. Membrane preparation (2 μg of α_{1B}-AR, α_{1D}-AR and 5 μg of α_{1A}-AR in each well) was incubated with 1 nM [³H]-prazosin, and these probes (10 points, threefold dilution from 10 μM) in were kept in 96-well polypropylene plates with assay buffer at 37 °C for 2 h, in which phenylephrine (J&K) was used as positive control. The competition curves are depicted in Figure S3A.

Calcium Flux Assay. The calcium flux experiments were conducted using α_{1A}-, α_{1B}-, and α_{1D}-ARs stable transfected HEK293 cells. Cells were plated in a Matrigel-coated 384-well black plate with a density of 2×10^4 in each well. After incubating for 20−24 h, the medium was carefully removed, the 1× Fluo-8 dye-loading solution was added in 40 μL to each well and then incubated at room temperature in the dark for 90 min. A series of concentrations of these fluorescent agonists (10 points, threefold dilution from 10 μM) were prepared in 1× HBSS and 10 mM HEPES mixture and then was added into compound plate with 10 μL in each well. The plate was read by a Molecular Devices FlexStation3 microplate reader in 90 s readout duration, with one time of compound transfer from compound plate to assay plate at 20 s.

Cytotoxicity Assay. CCK-8 assay was used to study the cell viability of α_{1A}-, α_{1B}-, and α_{1D}-ARs stably transfected and untransfected HEK293A cells exposed to **5a−c** and phenylephrine. After the cells (100 μL, 8×10^3 each well) were incubated in 96-well plates for 24 h, a series of twofold dilutions of probes in growth medium without FBS were added and incubated for another 24 h. Hereafter, the medium was removed , and the dye in growth medium without FBS was added. After incubation for 2 h, the absorbance values were recorded.

Assay of Specificity and Selectivity for α_1-ARs. All these experiments were determined with assay buffer (50 mM Tris-HCl, 10 mM KCl, 1 mM MgCl$_2$, pH 7.4) in 96-well black flat plates. The membrane preparation is described in the Supporting Information.

Measure of Specificity. The α_1-ARs membrane proteins of different concentrations (0, 0.0625, 0.125, 0.25, 0.5, and 1.0 mg/mL) were incubated with these probes (5 μM) at room temperature for 30 min, respectively. Then, the fluorescence emission spectra were measured by a PerkinElmer EnSpire microplate reader (λ_{ex}: 480 nm).

Selectivity of α_1-ARs. The α_1-AR membrane proteins (0.5 mg/mL), BSA (1 mg/mL), α-chymotrypsin (1 mg/mL), papain (1 mg/mL), pepsin (1 mg/mL), and trypsin (1 mg/mL) were incubated with these probes (1 μM) at room temperature for 30 min, respectively. Then, the fluorescence intensity at 550 nm was recorded with excitation wavelength at 480 nm by a PerkinElmer EnSpire microplate reader.

Fluorescence Polarization Assay. All these experiments were performed on the 384-well flat bottom black plates (Fluotrac 600, Greiner Bio-One Ltd., Stonehouse, U.K.) in 50 mM Tris-HCl, 5 mM MgCl$_2$, and 1 mM CaCl$_2$ solution. The α_1-ARs proteins of a series concentration were treated with 5 μM probes at room temperature for 1 h. In addition, the indicated concentrations of these probes (0, 0.156, 0.312, 0.625, 1.25, 2.5, 5.0 μM) were incubated with α_1-AR proteins (0.5 mg/mL) at room temperature for 1 h. Moreover, compound **5a** (5.0 μM) was incubated with α_1-AR proteins (0.5 mg/mL) at room temperature for the indicated time (60, 90, 120 min), and α_1-ARs membrane was exposed to room temperature for 1 h; subsequently, α_1-AR levels were analyzed by Western blotting (Figure S6). The fluorescent polarization

values were recorded in 550 nm emission with 485 nm excitation by a POLARstar Omega microplate reader (BMG LABTECH, Germany), and the K_d value was calculated.

Western Blot Analysis. Cells were lysed with ice in cold lysis buffer containing a protease inhibitor cocktail, and the protein concentrations of the extracts were tested by BCA assay. Equal volume and equal amounts of extracts were separated by SDS-PAGE electrophoresis and then were transferred onto nitrocellulose membranes. After blocking with 3% BSA, the blots were probed overnight at 4 °C with primary antibody for α_{1A}-AR (ab137123, Abcam), primary antibody for α_{1B}-AR (ab169523, Abcam), and primary antibody for α_{1D}-AR (sc-390884, Santa Cruz Biotechnology), respectively, in which primary antibodies of α_{1A}- and α_{1B}-ARs were diluted at a ratio of 1:1000, and that of α_{1D}-AR was diluted at a ratio of 1:500. Afterward, blots were washed and incubated with horseradish peroxidase-conjugated secondary antibody (Proteintech Group, Inc.). Bands were visualized by a chemiluminescence detection system (ChemiScope, Clinx). Autoradiographs were quantitated by the ImageJ software and were analyzed using the GraphPad Prism 7.

Fluorescence Imaging and Video Capture in Living Cells. All the cells were grown in the DMEM with 10% (v/v) fetal bovine serum (FBS) at 37 °C, 5% CO$_2$. Before imaging, the cells were plated in a confocal dish for at least 24 h and then washed three times with PBS buffer (pH 7.4) carefully. Compound **5a−c** solutions were prepared in growth medium DMEM without FBS. After incubation for 10 min in α_1-AR stable-transfected and nontransfected cells at room temperature with the indicated concentration of probes without or with 10-fold tamsulosin, the cells were imaged by a Zeiss Observer A1 microscope. Meanwhile, DID and Hochest dyes were coincubated. All obtained images were adjusted by the ImageJ software. In addition, HEK293 cells expressing α_{1A}- and α_{1B}-AR treated with these probes were immediately traced by a LSM780 confocal microscopy in a real-time manner at interval of 30 s.

Building and Application of BRET Assay. HEK293 cells stably expressing α_1-ARs tagged with the *Renilla* luciferase (RLuc) were well established. The three membrane proteins of RLuc-α_1-ARs-HEK 293 cells were prepared in assay buffer as in the above method. For saturation binding experiment, the membrane proteins (0.2 mg/mL) were incubated with the indicated concentration of compound **5a** (for α_{1A}- and α_{1B}-ARs) and **5c** (for α_{1D}-AR) at room temperature for 1 h in the presence of 10-fold tamsulosin as nonspecific binding. Subsequently, coelenterazine CTZ (50 μM) was added in assay buffer, and the bioluminescence intensity was measured in 485 and 550 nm emission after 5 min incubation at room temperature by a POLARstar Omega microplate reader (BMG LABTECH, Germany), and the K_d value was calculated. The Net mBRET was generated after multiplying the ratio of 545/460 by 1000. For application experiment, fluorescent ligand **5a** (3 μM of α_{1A}-AR and 6 μM of α_{1B}-AR) and **5c** (1.5 μM of α_{1D}-AR) and the indicated concentration of α_1-AR agonists or antagonists were incubated with three RLuc-α_1-ARs membrane proteins (0.2 mg/mL) for 1 h at room temperature. The bioluminescence intensity was recorded after addition of CTZ (50 μM) and 5 min incubation. All data were adjusted using Graphpad Prism v7 with one-site binding model. The obtained IC$_{50}$ and K_i value of three α_1-AR subtypes, and the comparison with that published in references by radio-ligand binding assay,

Table 1. Spectroscopic Properties and Receptor Binding and Functional Activities[a]

					$K_i{}^d$/(μM)			EC50[e]/(μM)		
probe	λ_{ex}	λ_{em}	SS[b]	Φ[c]	α_{1A}-AR	α_{1B}-AR	α_{1D}-AR	α_{1A}-AR	α_{1B}-AR	α_{1D}-AR
5a	480 nm	550 nm	70 nm	0.05	0.58 ± 0.06	>10	0.20 ± 0.00	>10	>10	>10
5b	480 nm	550 nm	70 nm	0.05	1.40 ± 0.08	>10	0.45 ± 0.01	>10	>10	>10
5c	480 nm	550 nm	70 nm	0.06	1.57 ± 0.28	>10	0.27 ± 0.03	>10	1.816	2.778
PE	NT	NT	NT	NT	2.33 ± 0.13	>10	2.12 ± 0.24	0.062	0.034	1.414

[a]NT, not tested. [b]SS, Stokes shift. [c]Φ, absolute quantum yield in PBS buffer. [d]K_i value was obtained from radio-ligand competitive binding assay (Data are means ± SEM, $n = 2$). [e]EC50 was obtained from calcium flux assay ($n = 1$).

are displayed in Table 2. A concentration-dependent manner with sigmoidal response curves is displayed in Figure S11.

■ RESULTS AND DISCUSSION

Spectroscopic and Pharmacologic Properties. First, the fluorescent properties of these fluorescent agonists including UV absorption and fluorescence spectra as well as quantum yields were determined as summarized in Table 1 (see details in Figure S1).

As expected, these probes displayed maximum UV absorption at 487 nm and fluorescent emission wavelength in green-range at 550 nm (excitation wavelength at 480 nm) with Stokes shift of 70 nm. The quantum yields were also observed up to 6%. To preliminary detect the environment-sensitive properties, the fluorescence spectra of these compounds in different polarity and viscosity are also recorded (Figure S1) for emulating the hydrophobic receptor ligand-binding site environment. Significant fluorescent intensity decrease was observed in the aqueous solution (PBS or water) compared with that in organic solvents. For example, compound **5a** displayed approximately 30-fold fluorescence enhancement in PBS buffer compared with acetonitrile solution (Figure 1A). Moreover, the fluorescence was
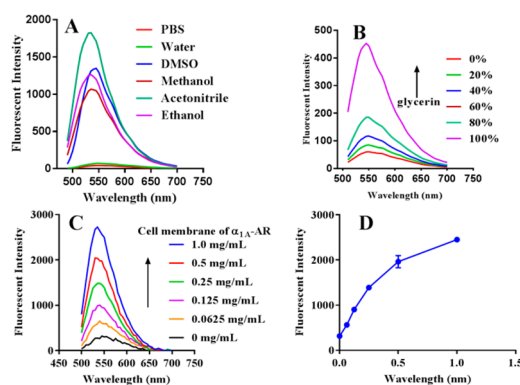

Figure 1. Emission spectra of **5a** obtained in different polarity solvents (A) and in a mixture of glycerin and water by indicating with % v/v (B). Fluorescence emission spectra of 5 μM **5a** incubated with different concentrations α_{1A}-ARs membrane proteins for 30 min (C) and fluorescence intensity at the 550 nm of emission (D) (Data are mean ± SEM, $n = 2$).

dramatically heightened with the increasing viscosity in the mixture of glycerin and water, such as about sevenfold increase of fluorescence was found of compound **5a** with glycerin volume fraction increasing from 0 to 100% when viscosity gradually increased (Figure 1B). These results clearly suggested the fluorescent change upon varying surrounding environment polarity and viscosity.

Radio-Ligand Competitive Binding Assay to α_1-ARs. To test the binding affinity to α_1-ARs, theses targeted compounds were first evaluated by a radio-ligand competitive binding assay with [³H] prazosin in membrane from the human α_{1A}-, α_{1B}-, and α_{1D}-ARs transfected HEK293 cells. As shown in Table 1, Figures S3A, and Table S1, all probes exhibited almost equivalent even higher affinity to three α_1-AR subtypes compared with phenylephrine. This would be that the introduction of fluorophore-NBD may change conformation to show prevailing structure−activity relationship with α_1-ARs on the basis of the Easson−Stedman hypothesis.[33] Moreover, it can be found that compound **5a** containing eight carbon atoms of linker displayed a higher binding affinity to α_1-ARs than compounds **5b** and **5c** which had a linker with six or four carbon atoms, respectively; however to α_{1B}-AR, compound **5c** showed better binding affinity. These results demonstrate that the modification of phenolic hydroxyl of phenylephrine with fluorophore NBD through a linker of four, six, or eight carbon atoms has almost no negative influence on the binding affinity. Hence, these fluorescent agonists can be selected in the following further activity evaluation experiment.

Functional Characterization by Calcium Flux Assay. Initial functional characterization of these fluorescent agonists was determined by calcium flux assay in HEK293 cells that express α_{1A}-, α_{1B}-, and α_{1D}-ARs (Table 1 and Figure S3B). As the results show, the obviously reduced potency was observed compared to the parent compound phenylephrine. This indicated that the inker length may impact their functional interaction with α_1-ARs.

Cytotoxicity Assay. It should be noted that the low cytotoxicity is important for a reasonable probe labeling the GPCR. Herein, a CCK-8 assay was performed to evaluate the cytotoxicity of these fluorescent agonists **5a−c** with phenyl-ephrine as the control. Four cell lines including α_{1A}-, α_{1B}-, and α_{1D}-ARs stable transfected HEK293 cells and normal HEK293 cell were selected to detect. As depicted in Table S2, all compounds exhibited a micromolar level of cytotoxicity in all these four cell lines, while showing slight difference compared to phenylephrine. Overall, the biocompatibility of these molecules to living cells under the experimental conditions allowed these compounds to be used for detecting and imaging α_1-ARs in living cells.

Specificity and Selectivity for α_1-AR. As discussed above, these fluorescent agonists were proposed to have environment-sensitive turn-on mechanism and be selectivity recognized. To validate this hypothesis, these compounds (5 μM) were incubated with a series of concentrations of α_1-ARs transfected HEK293 membrane proteins for 30 min, respectively, and then the corresponding fluorescence intensity was recorded. As expected, significant fluorescence enhance-ment was obtained (Figures S4). When **5a** was incubated with increasing membrane proteins up to 1.0 mg/mL, the
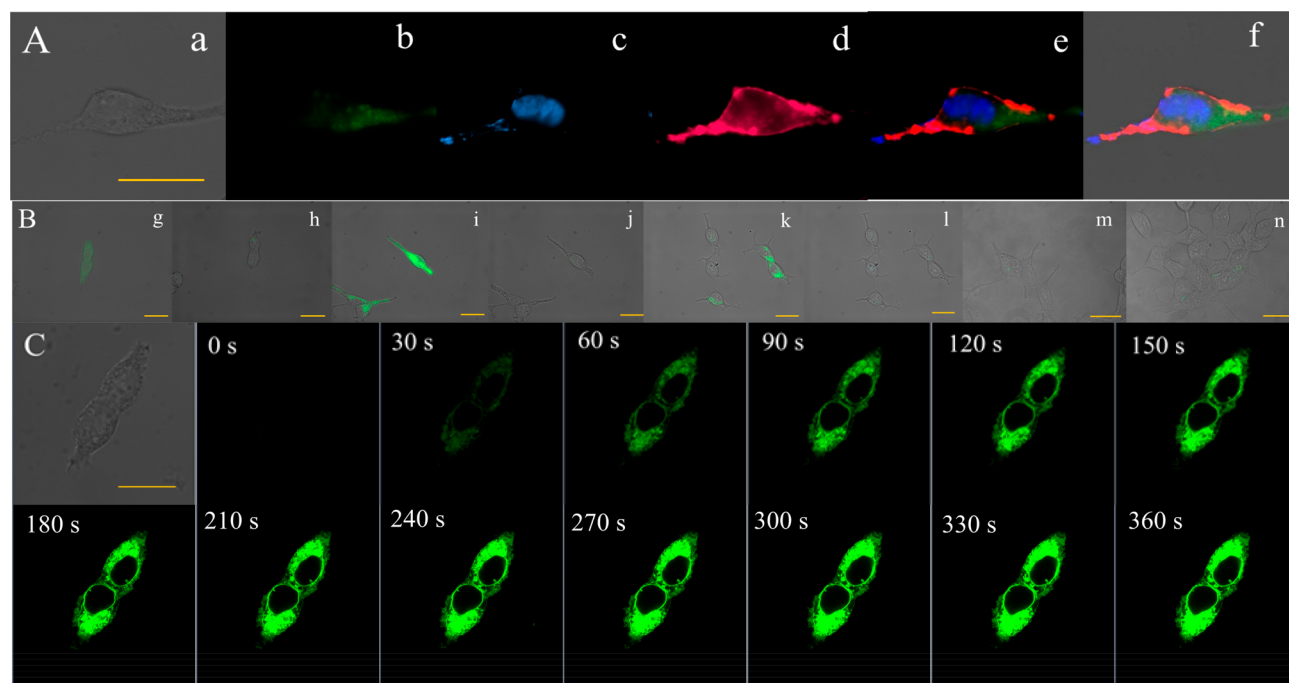
Figure 2. (A) Fluorescence colocalization imaging of α_{1A}-ARs transfected HEK293 cells incubated with 250 nM of **5a** (a, bright field; b, green channel indicated florescence of probe **5a**; c, blue channel indicated florescence of Hoechst dye; d, red channel indicated florescence of DID dye; e, color merged image; f, merged image) and (B) fluorescence imaging of **5a** without (g, i, k) or with (h, j, l) 10-fold tamsulosin of α_1-ARs transfected HEK293 cells and nontransfected HEK293 (100 nM of m, 250 nM of n) using a Zeiss Observer A1 microscopye. g, h: α_{1A}-AR (250 nM); i, j: α_{1B}-AR (100 nM); k, l: α_{1D}-AR (100 nM). (C) Fluorescence real-time imaging of α_{1B}-AR transfected HEK293A cells with **5a** (1.25 μM) was observed in an interval of 30 s without washing on a LSM780 confocal microscope. Scale bar = 20 μm.

fluorescence intensity increased approximately 10-fold for α_1-ARs three subtypes compared with the blank group (Figure 1C, 1D). Additionally, when these probes were evaluated in assay buffer (50 mM Tris-HCl, 1 mM MgCl$_2$, 10 mM CaCl$_2$, pH 7.4), their maximum emission wavelength showed blue-shift about 15 nm after adding membrane proteins. Moreover, similar environment-sensitive properties were observed while conducting the measurement in different solvents with various polarities.

Based on these encouraging results, the selectivity enhancement of fluorescent intensity for α_1-ARs was examined, in which other five proteins including BSA, chymotrypsin, papain, pepsin, and trypsin were chosen as negative controls. As shown in Figure S4E, when treated with three membrane proteins of α_1-ARs subtypes, these compounds (5 μM) showed about 10-fold fluorescence increases as compared to 2-fold excess of the other five proteins.

Fluorescence Polarization Assay. The fluorescence polarization (FP) assay has many advantages including being nonradioactive, without tedious steps, and self-referencing, as well as low-cost.[17,34] Polarization value is defined as the ratio of fluorescence intensities parallel ($I_\parallel$) and perpendicular ($I_\perp$) with respect to the plane-polarized excitation light.[17,35] Generally speaking, freely moving fluorophores with fast rotation will disturb polarization, whereas the constrained fluorophores will exhibit stronger polarized fluorescence after binding to receptors.[17,28,35] In order to study the receptor binding affinity, a FP assay was performed to test the binding affinity of α_1-ARs with these fluorescent agonists based on the changes of their fluorescent properties. It can be found that FP values of compounds **5a−c** (5 μM) were gradually enhanced with the increasing of three α_1-ARs membranes concentrations.

Meanwhile, FP value presented a dose-dependent enhancement when a series of concentrations of molecules **5a−c** were incubated with 0.5 mg/mL membrane proteins (Figure S5), as shown in Figure 3 for **5a**, and K_d value was calculated (Table S3). The results revealed a highly sensitive response toward α_1-ARs of these new probes, which indicated an efficient binding profile.
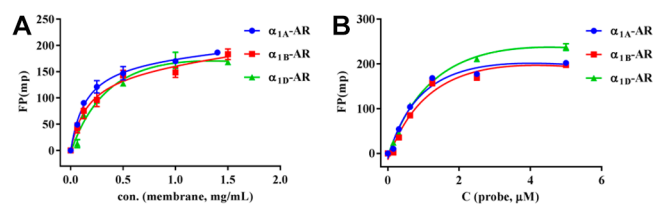

Figure 3. Fluorescence polarization (FP) assay tested the interaction between **5a** (5 μM) and different concentrations of α_1-ARs membrane (A) and fluorescent polarization value response to the concentration increase of probes at 0.5 mg/mL membrane (B). Data are mean ± SEM, $n = 2$.

α_1-ARs Internalization Induced by Fluorescent Agonist. As some studies show, when GPCRs were stimulated with corresponding agonists, the mechanism of internalization could be induced. We attempted to explore whether our fluorescent agonists can induce the internalization of α_{1A}-AR which could be distributed in both cell membrane and cytoplasm, and α_{1B}-AR which mainly distributed on cell membrane. After treating α_{1A}- and α_{1B}-ARs stable transfected HEK293 cell with compound **5a**, respectively, we examined the level of α_{1A}- and α_{1B}-ARs in cytoplasm by Western blot assay. As shown in Figure S7, compounds **5a** induced a time-

dependent and dose-dependent increase of α_{1A}- and α_{1B}-ARs in cytoplasm. These results suggested that compound **5a** could still induce the internalization of α_{1A}- and α_{1B}-ARs.

Visualizing Human α_1-ARs and Receptor Internalization on Living Cells. *Localization Imaging.* The α_1-ARs imaging studies using all these probes in living cells were conducted. The stable α_1-ARs transfected HEK293 cells as positive groups were incubated with **5a** for 10 min at room temperature and in the presence of tamsulosin as negative groups. DID, a cell membrane dye with red florescence, and Hoechst, a nucleus dye with blue florescence, were used for colocalization. It was found that **5a** could selectively label α_{1A}-, α_{1B}-, and α_{1D}-AR transfected HEK293 cells (Figure 2A, S8), while the fluorescence decreased upon adding a 10-fold excess of antagonist tamsulosin, and nontransfected HEK293 showed only slight fluorescence (Figure 2B). As shown in Figure S9, the emission spectra and fluorescence intensity of compound **5a** were not obviously affected with the 10-fold antagonist tamsulosin in PBS buffer and acetonitrile. The imaging results confirmed that these environment-sensitive agonists have favorable selectivity for α_1-ARs three subtypes and could be applied to locate the α_1-ARs.

Monitoring Internalization of α_1-ARs. Based on the Western blotting and imaging results described above, we further investigated whether our fluorescent agonists can be used for tracing the α_{1A}-AR internalization by real-time confocal video (see Supporting Information Videos S1, S2, S3, S4, S5, and S6), and the real-time imaging is exhibited in Figure S10. After adding these probes, the stable α_{1A}-AR and α_{1B}-AR transfected HEK293 cells were tested immediately without a complex washing. It can be found that the fluorescence movement was happening and the fluorescence region in cytoplasm gradually expanded, and additionally the cell membrane region became slightly uneven for α_{1A}-and α_{1B}-ARs transfected HEK293. This is similar to the results obtained from the above location imaging and the corresponding imaging of **5a** for α_{1B}-AR as shown in Figure 2C. The result indicated that our fluorescent agonists could induce α_{1A}-and α_{1B}-AR internalization, meanwhile with real-time monitoring of this internalization dynamic process with one self fluorescent signal.

BRET Assay Based on Synthetic Fluorescent Agonists. Encouraged by these results described above, a binding assay utilizing these fluorescent ligands as a tracer and based on a bioluminescence resonance energy transfer (BRET) approach was conducted. BRET assay depends on energy transfer between a bioluminescent donor and fluorescent acceptor, which is also useful for real-time monitoring interaction between GPCRs and ligands.[36] For this, α_1-ARs were tagged with *Renilla* luciferase (RLuc) expressed in HEK293 cell. RLuc is a bioluminescent enzyme[37] and can oxidize its substrates and exhibit an emission spectrum, which has excellent overlap with the excitation spectrum of NBD. Moreover, coelenterazine (CTZ) was selected as the substrate of RLuc.[38] Therefore, when our probes bound to RLuc-α_1-ARs, energy transfer at 480 nm between the RLuc and NBD moiety happened after adding CTZ, and then NBD of these probes demonstrated emission at 550 nm (Figure 4). To explore a saturation binding experiment, varying concentrations of these probes were incubated with three membrane proteins in 0.2 mg/mL of RLuc-α_1-ARs, respectively, and nonspecific binding was determined in the presence of 10-fold excess for tamsulosin. Herein, compound **5a** was chosen as a tracer of α_{1A}- and α_{1B}-
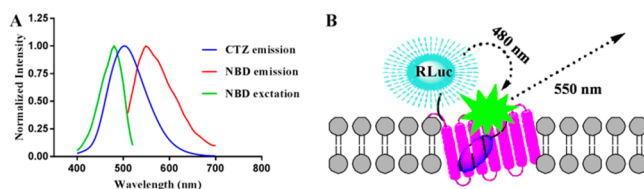

Figure 4. (A) Emission spectrum of CTZ upon stimulating RLuc and the excitation and emission spectra of compound **5**. (B) Illustration of the design concept of the BRET assay using compound **5** and RLuc. Upon binding to receptor and then stimulating with CTZ, the receptor-bound RLuc emitted at 480 nm and through BRET transferred to the fluorophore, resulting in emission at 550 nm.

ARs; however, **5c** was selected for α_{1D}-AR, on the basis of their fluorescent properties, binding affinities, and above so on. In addition, the Net mBRET was used to respond to BRET activity, and the calculated K_d values are displayed (1.81 ± 0.29 μM of α_{1A}-AR, 2.71 ± 1.25 μM of α_{1B}-AR, and 0.71 ± 0.16 μM of α_{1D}-AR) (Figure 5). This result suggested that our probes can effectively respond to α_1-ARs based on BRET.
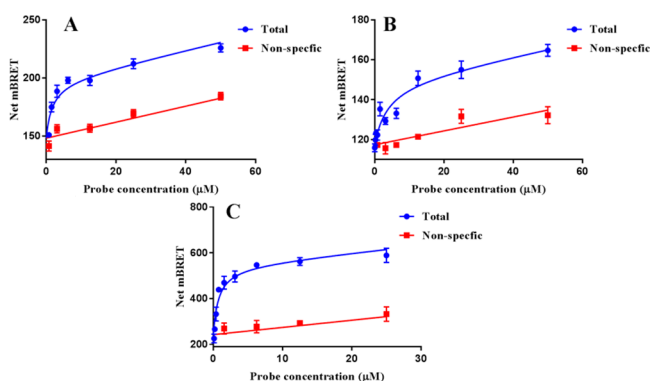

Figure 5. Representative saturation binding experiment tested with α_{1A}-AR (A), α_{1B}-AR (B), and α_{1A}-AR (C). Nonspecific binding was defined in the presence of 10-fold tamsulosin (λ_{em}: 550 nm, λ_{ex}: 485 nm). Data are mean $\pm$ SEM, $n = 3$.

Next, we further tested whether this BRET-based strategy could be used in high-throughput screening (HTS) for previously published α_1-AR agonists or antagonists. Competition binding assays were also conducted in the presence of **5a** (3 μM of α_{1A}-AR and 6 μM of α_{1B}-AR) or **5c** (1.5 μM of α_{1D}-AR) and three RLuc-α_1-ARs membrane proteins in 0.2 mg/mL. As known competitive α_1-AR ligands, agonists including methoxamine, norepinephrine, and epinephrine and antagonists such as prazosin, tamsulosin, phentolamine, and doxazosin both could reduce mBRET in a concentration-dependent manner with sigmoidal response curves (Figure S11). In Table 2, the obtained IC_{50} and K_i values of three α_1-AR subtypes were exhibited, and some of these values were similar to radio-ligand binding values in the literature.[39−45] According to these results, after further study, our fluorescent agonists maybe could serve as a fluorescent tracer for BRET-based binding assay which can be used for HTS of α_1-ARs chemical library.

■ CONCLUSION

In this study, we have developed a series of novel fluorescent agonists on the basis of "off−on" mechanism for α_1-ARs with low background signal using environment-sensitive small

Table 2. Comparison of Binding Affinity Results in BRET Assay to Reference Data

compds	BRET IC$_{50}$[a] (nM)			BRET K_i[b] /(nM)			ref K_i[c] /(nM)		
	α_{1A}-AR	α_{1B}-AR	α_{1D}-AR	α_{1A}-AR	α_{1B}-AR	α_{1D}-AR	α_{1A}-AR	α_{1B}-AR	α_{1D}-AR
methoxamine	1.64 ± 0.28	38.3 ± 9.00	1.47 ± 0.23	0.62 ± 0.11	11.9 ± 2.80	0.55 ± 0.40	5.50	97.72	12.30
norepinephrine	12.0 ± 0.80	1.13 ± 0.36	0.12 ± 0.03	4.53 ± 0.30	0.35 ± 0.11	0.04 ± 0.01	1.02	0.69	0.04
epinephrine	3.89 ± 0.83	3.10 ± 1.06	0.11 ± 0.04	1.47 ± 0.31	0.97 ± 0.33	0.04 ± 0.01	0.40	0.30	0.05
doxazosin	0.50 ± 0.26	1.61 ± 0.38	0.70 ± 0.37	0.19 ± 0.09	0.50 ± 0.12	0.23 ± 0.11	3.16	1.00	4.00
prazosin	0.97 ± 0.41	1.33 ± 0.37	0.71 ± 0.68	0.37 ± 0.16	0.26 ± 0.08	0.23 ± 0.22	0.20	0.25	0.32
phentolamine	0.17 ± 0.03	10.5 ± 5.32	2.76 ± 1.08	0.07 ± 0.01	3.26 ± 1.66	0.89 ± 0.35	1.60	7.90	7.90
tamsulosin	1.16 ± 0.14	8.55 ± 1.96	1.39 ± 0.72	0.44 ± 0.05	2.66 ± 0.60	0.45 ± 0.23	0.004	0.10	0.008

[a]IC$_{50}$ values were tested by the competitive binding based on established BRET assay. [b]K_i values were tested by the competitive binding based on established BRET assay. [c]K_i values were acquire from radio-ligand binding assay as references published. Data are mean ± SEM, n = 3.

fluorophore NBD. These new fluorescent agonists are easy to prepare. After binding to α_1-ARs, the hydrophobic binding domain induced strong fluorescence release. Among these fluorescent agonists, compound **5a** possessed outstanding spectroscopic properties and acceptable binding as well as obvious fluorescence enhancement about 10-fold upon binding to α_1-ARs. The analytical method FP assay has been successfully identified based on the interactions between these compounds and α_1-ARs. These fluorescent agonists can be a useful fluorescent turn-on tool for selective and specific labeling of α_1-ARs in living cells. It is worth mentioning that these probes also successfully trace the all dynamic process of receptor internalization. Moreover, the BRET-based binding assay with fluorescent ligand **5a** or **5c** has also been successfully established which is suitable for high-throughput competition binding screening research of unlabeled α_1-ARs ligands including various agonists and antagonists, comparable to those obtained from previous reports using radio-label ligands. It is expected that these versatile environment-sensitive fluorescent agonists can be utilized to greatly extend toolboxes for molecular pharmacology and drug discovery of α_1-ARs.

■ ASSOCIATED CONTENT

ⓈSupporting Information

The Supporting Information is available free of charge on the ACS Publications website at DOI: 10.1021/acs.anal-chem.9b01059.

Optical spectra in different solvents, membrane titration and saturation binding, binding affinity IC$_{50}$ and curves, functional concentration−response curves, cytotoxicity results, fluorescence turn-on emission spectra, fluorescence polarization saturation curves and K_d values, α_1-ARs stable in room temperature, internalization by Western blotting, cell colocalization imaging results of compound **5a**, how tamsulosin affects the native fluorescence of **5a**, fluorescence real-time imaging, competition curves based on established BRET assay, ^{1}H NMR, ^{13}C NMR, MS, HRMS, and HPLC data (PDF)

Fluorescence real-time video of α1A-AR with 1.25 μM **5a** (generated with 30 s interval) (AVI)

Fluorescence real-time video of α1B-AR with 1.25 μM **5a** (generated with 30 s interval) (AVI)

Fluorescence real-time video of α1A-AR with 2.5 μM **5b** (generated with 30 s interval) (AVI)

Fluorescence real-time video of α1B-AR with 1.25 μM **5b** (generated with 30 s interval) (AVI)

Fluorescence real-time video of α1A-AR with 2.5 μM **5c** (generated with 30 s interval) (AVI)

Fluorescence real-time video of α1A-AR with 2.5 μM **5c** (generated with 30 s interval) (AVI)

■ AUTHOR INFORMATION

Corresponding Author
*Phone/fax: +86-531-8838-2076. E-mail: mli@sdu.edu.cn.

ORCID
Xiaodong Shi: 0000-0002-3189-1315
Lupei Du: 0000-0003-0531-8985
Minyong Li: 0000-0003-3276-4921

Author Contributions
The manuscript was written through contributions of all authors.

Notes
The authors declare no competing financial interest.

■ REFERENCES

(1) Yang, J.; Yan, Y.; Xiang, X.; Xu, Y.; Zhou, N.; Wang, T. *J. Vis. Exp.* **2017**, *122*, 1−7.
(2) Wang, S. Y.; Song, Y.; Xu, M.; He, Q. H.; Han, Q. D.; Zhang, Y. Y. *Acta Pharmacol. Sin.* **2007**, *28*, 359−366.
(3) Ma, Z.; Lin, Y.; Cheng, Y.; Wu, W.; Cai, R.; Chen, S.; Shi, B.; Han, B.; Shi, X.; Zhou, Y.; Du, L.; Li, M. *J. Med. Chem.* **2016**, *59*, 2151−2162.
(4) Liu, T.; Gao, Y.; Zhang, X.; Wan, Y.; Du, L.; Fang, H.; Li, M. *Anal. Chem.* **2017**, *89*, 11173−11177.
(5) Liu, Z.; Wang, B.; Ma, Z.; Zhou, Y.; Du, L.; Li, M. *Anal. Chem.* **2015**, *87*, 2550−2554.
(6) Liu, Z.; Jiang, T.; Wang, B.; Ke, B.; Zhou, Y.; Du, L.; Li, M. *Anal. Chem.* **2016**, *88*, 1511−1515.
(7) Bunnage, M. E.; Chekler, E. L.; Jones, L. H. *Nat. Chem. Biol.* **2013**, *9*, 195−199.
(8) Liu, Z.; Du, L.; Li, M. *Sci. China: Chem.* **2013**, *56*, 1667−1670.
(9) Ma, Z.; Du, L.; Li, M. *J. Med. Chem.* **2014**, *57*, 8187−8203.
(10) Leopoldo, M.; Lacivita, E.; Berardi, F.; Perrone, R. *Drug Discovery Today* **2009**, *14*, 706−712.
(11) Zhuang, Y. D.; Chiang, P. Y.; Wang, C. W.; Tan, K. T. *Angew. Chem., Int. Ed.* **2013**, *52*, 8124−8128.

(12) Zhong, H.; Minneman, K. P. *Eur. J. Pharmacol.* **1999**, *375*, 261−276.

(13) Koshimizu, T.-a.; Tanoue, A.; Hirasawa, A.; Yamauchi, J.; Tsujimoto, G. *Pharmacol. Ther.* **2003**, *98*, 235−244.

(14) Docherty, J. R. *Cell. Mol. Life Sci.* **2010**, *67*, 405−417.

(15) Kojima, Y.; Sasaki, S.; Hayashi, Y.; Tsujimoto, G.; Kohri, K. *Nat. Clin. Pract. Urol.* **2009**, *6*, 44−53.

(16) Li, W.; Du, L.; Li, M. *Curr. Med. Chem.* **2011**, *18*, 4923−4932.

(17) Ma, Z.; Liu, Z.; Jiang, T.; Zhang, T.; Zhang, H.; Du, L.; Li, M. *ACS Med. Chem. Lett.* **2016**, *7*, 967−971.

(18) Zhang, W.; Ma, Z.; Li, W.; Li, G.; Chen, L.; Liu, Z.; Du, L.; Li, M. *ACS Med. Chem. Lett.* **2015**, *6*, 502−506.

(19) Lin, Y.; Li, W.; Yu, Q.; Zhou, X.; Zhang, W.; Du, L.; Li, M. *Sci. China: Chem.* **2016**, *59*, 624−628.

(20) Zhang, W.; Zhou, X.-Y.; Yu, Q.-Y.; Du, L.-P.; Li, M.-Y. *Chin. Chem. Lett.* **2016**, *27*, 185−189.

(21) Fonseca, M. I. B.; Button, D. C.; Brown, R. D. *J. Biol. Chem.* **1995**, *270*, 8902−8909.

(22) Bishop, M. *Curr. Top Med. Chem.* **2007**, *7*, 135−145.

(23) Christiansen, E.; Hudson, B. D.; Hansen, A. H.; Milligan, G.; Ulven, T. *J. Med. Chem.* **2016**, *59*, 4849−4858.

(24) Hansen, A. H.; Sergeev, E.; Pandey, S. K.; Hudson, B. D.; Christiansen, E.; Milligan, G.; Ulven, T. *J. Med. Chem.* **2017**, *60*, 5638−5645.

(25) Toyo'oka, T. W.; Watanabe, Y.; Imai, K. *Anal. Chim. Acta* **1983**, *149*, 305−312.

(26) Lin, S. S.; Struve, W. S. *Photochem. Photobiol.* **1991**, *54*, 361−365.

(27) Uchiyama, S. S.; Santa, T.; Imai, K. *J. Chem. Soc., Perkin Trans.* **1999**, *11*, 2525−2532.

(28) Banks, P.; Prystay, L.; Gosselin, M. *J. Biomol. Screen.* **2000**, *5*, 159−167.

(29) Jones, J. W.; Greene, T. A.; Grygon, C. A.; Doranz, B. J.; Brown, M. P. *J. Biomol. Screening* **2008**, *13*, 424−429.

(30) Kool, J.; van Marle, A.; Hulscher, S.; Selman, M.; van Iperen, D. J.; van Altena, K.; Gillard, M.; Bakker, R. A.; Irth, H.; Leurs, R.; Vermeulen, N. P. *J. Biomol. Screening* **2007**, *12*, 1074−1083.

(31) Newman-Tancredi, A.; Cussac, D.; Audinot, V.; Gavaudan, S.; Millan, M.; Pasteau, V. *Mol. Pharmacol.* **1999**, *55*, 564−574.

(32) Lane, J. R.; Powney, B.; Wise, A.; Rees, S.; Milligan, G. *J. pharmacology and experimental therapeutics* **2008**, *325*, 319−330.

(33) Patil, P. N.; Li, C.; Kumari, V.; Hieble, J. P. *Chirality* **2008**, *20*, 529−543.

(34) Singleton, D. H.; Steidl-Nichols, J. V.; Deacon, M.; Groot, M. J.; Price, D.; Nettleton, D. O.; Wallace, N. K.; Troutman, M. D.; Williams, C.; Boyd, J. G.; Boyd, H. *J. Med. Chem.* **2007**, *50*, 2931−2941.

(35) Jia, T.; Fu, C.; Huang, C.; Yang, H.; Jia, N. *ACS Appl. Mater. Interfaces* **2015**, *7*, 10013−10021.

(36) Stoddart, L. A.; Johnstone, E. K. M.; Wheal, A. J.; Goulding, J.; Robers, M. B.; Machleidt, T.; Wood, K. V.; Hill, S. J.; Pfleger, K. D. G. *Nat. Methods* **2015**, *12*, 661−663.

(37) Jiang, T.; Du, L.; Li, M. *Photochem. Photobiol. Sci.* **2016**, *15*, 466−480.

(38) Jiang, T.; Yang, X.; Zhou, Y.; Yampolsky, I.; Du, L.; Li, M. *Org. Biomol. Chem.* **2017**, *15*, 7008−7018.

(39) Foglar, R.; Horie, K.; Hirasawa, A.; Tsujimoto, G.; Shibata, K. *Eur. J. Pharmacol.* **1995**, *288*, 201−207.

(40) Bremner, J. B.; Coban, B.; Griffith, R.; Groenewoud, K. M.; Yates, B. F. *Bioorg. Med. Chem.* **2000**, *8*, 201−214.

(41) Kenny, B. A. M.; Miller, A. M.; Williamson, I. J. R.; O'Connell, J.; Chalmers, D. H.; Naylor, A. M. Br. *J. Pharmacol.* **1996**, *118*, 871−878.

(42) Obika, K.; Shibata, K.; Horie, K.; Foglar, R.; Kimura, K.; Tsujimoto, G. *Eur. J. Pharmacol.* **1995**, *291*, 327−334.

(43) Hwa, J.; Perez, D. M.; Graham, R. M. *J. Biol. Chem.* **1995**, *270*, 23189−23195.

(44) Van der Graaf, P. H.; Black, J. W. *J. Pharmacol.* **1996**, *118*, 876−883.

(45) Buckner, S. A.; Morse, P. A.; Knepper, S. M.; Hancock, A. A.; Oheim, K. W. *Eur. J. Pharmacol.* **1996**, *297*, 241−248.